Compact Metasurface Loaded Antenna with Improved Axial Ratio Beamwidth for Airborne Applications at 2.2 GHz

Mohammad Ameen*[(1)] and Raghvendra Kumar Chaudhary[(2)]
[(1),(2)]Department of Electronics Engineering, Indian Institute of Technology (Indian School of Mines), Dhanbad-826004, India
[(1)]mohammadmn61@gmail.com, and [(2)]raghvendra.chaudhary@gmail.com

Abstract

The proposed work explains a compact epsilon-negative (ENG) transmission line (TL) radiator antenna combined with metasurface (MS) reflector applicable for airborne applications at 2.2 GHz. The radiator antenna supports circular polarization radiation due to the combination of third-iterative fractal (TIF) and ENG-TL. The final MS reflector loaded antenna provides a smaller dimension of $0.46\lambda_0 \times 0.46\lambda_0 \times 0.011\lambda_0$ at 2.2 GHz. The antenna offers an acceptable impedance bandwidth (IBW) of (2.16–2.253 GHz) 4.22%, improved gain of 6.33 dBic, higher gain-to-area (G/A) ratio of 19.9 dB, extended axial ratio beamwidth of 100^0 and gain more than 2.04 dBic for $\theta = \pm 50^0$ and $\phi = 0^0$ to 360^0 at 2.23 GHz. Hence the presented MS reflector loaded antenna is suitable for airborne applications.

1 Introduction

Presently, wireless communication applications are targeting towards compact antennas with enhanced performance. The metamaterial (MTM) based TL antennas are the appropriate candidate to obtain antenna miniaturization [1]. The current system also focuses on circularly polarized (CP) antennas due to flexibility in the trans-receiver antennas placement and eliminating the losses that occur due to the ionosphere [1]. Various CP antennas designed using composite right/left-handed TL, ENG-TL, Mu-negative TL, and MTM inspired structures were presented in ref. [1]–[7]. These antennas use MTM inspired parasitic elements [3], fractal shaped defective ground structure [4], trimmed square ring and CRLH-TL based mushrooms [5], combination of CSRR and CRLH-TL [6], and combination of curved branches and ENG-TL based mushroom [7]. These above-reported designs are complicated in design due to the larger antenna size and occupancy of shorted vias. These structures also provide narrow IBW, smaller axial ratio bandwidth (ARBW), and smaller or negative gain values in the working band.

To reduce the above explained antenna anomalies and boost the radiation performance, metasurface (MS) based structures can be incorporated with the radiator antenna explained above. Various types of multilayer antenna configuration are explained in [8]–[12]. These antenna configuration use circular-shaped arrays [8], crossed dipole combined with artificial magnetic conductor (AMC) based MS [9], cavity-backed annular slot antenna [10], printed dipoles [11], and dipole antenna combined with superstrate [12]. These antennas provide higher volume, lower gain,

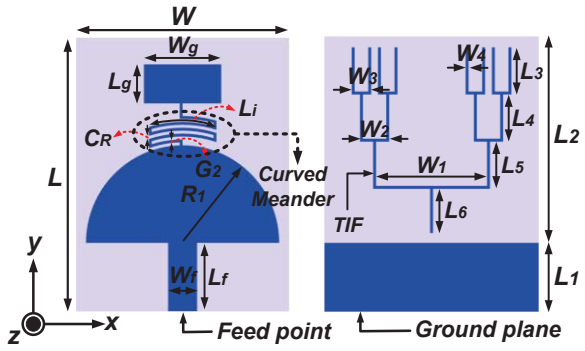

(a) (b)

Figure 1. Proposed ENG-TL based CP radiator antenna (a) Front view and (b) Back view.

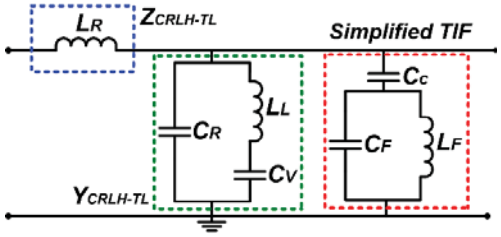

Figure 2. Approximate equivalent circuit diagram of the radiator antenna represented in Figure. 1

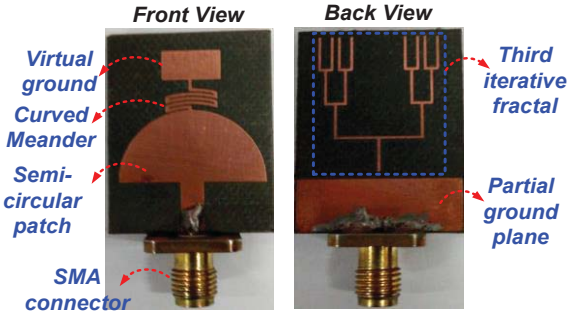

(a) (b)

Figure 3. Photograph of the fabricated ENG-TL radiator antenna. (a) Front view and (b) Back view.

and low G/A ratio which restricts the above-explained antennas in modern airborne application systems. Hence the proposed work mainly focuses on an ENG-TL based electrically small (ka = 0.65<1) radiator antenna, which is inspired from [13] is combined with newly designed MS reflector. The new MS reflector antenna provides lower antenna volume, improved gain, higher G/A ratio, extended AR beamwidth with no design complexity.

2 ENG-TL based Single Radiator Antenna

The schematic front-view and back-view of the intended ENG-TL based CP antenna is shown in Figure. 1(a) and (b). The presented ENG-TL radiator antenna is designed and fabricated on low loss Rogers 5880 substrate with ε_r = 2.2, tanδ = 0.0009 and thickness H_1 =1.58 mm. Figure. 2 shows the equivalent circuit model and Figure. 3 depicts the fabricated ENG-TL antenna. The antenna top layer is basically an ENG-TL unit cell comprised of a semicircular patch of radius R_1, which provides the series inductance (L_R). The shunt inductor (L_L) is represented by curved meander line of length L_i = 7 mm and width G_2 = 0.3 mm. The shunt capacitor (C_R) is denoted by the spacing between the meander line and coupling between the top-side ENG-TL layer and the partial ground plane. Finally, the curved meander line is directly connected to a rectangular-shaped stub for providing the virtual ground capacitor (C_V) [2]. For generating CP radiation, a TIF geometry is inserted in the backside which increases the cross-polarization level equivalent to the top ENG-TL antenna co-polarization level and generates CP radiation. The TIF is denoted by the

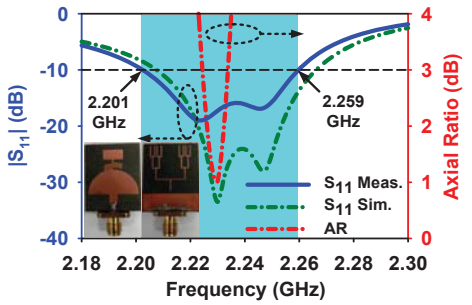

(a)

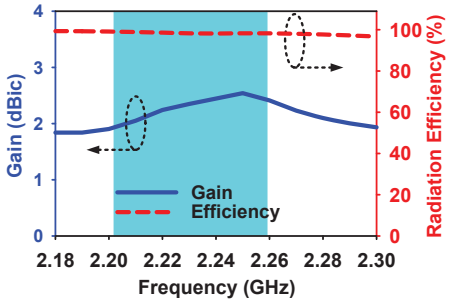

(b)

Figure 4. Proposed ENG-TL based CP radiator antenna results. (a) $|S_{11}|$ and AR, and (b) Gain and efficiency.

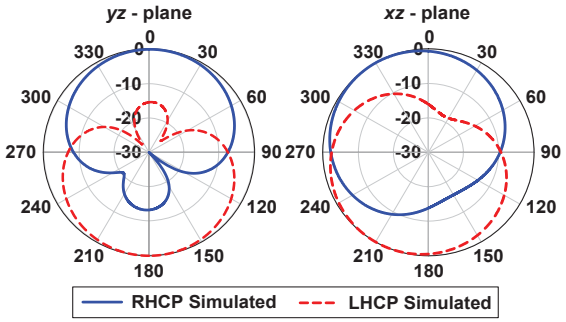

Figure 5. The 2D radiation patterns of the radiator antenna at *yz*-plane and *xz*-plane for 2.23 GHz.

Table 1. Comparison of the intended ENG-TL radiator antenna and existing TL based antennas.

Ref. No.	Freq. GHz	Electrical Size plane (λ_0^3)	IBW (%)	AR BW (%)	G/A Ratio (dB)	Via Process
[3]	1.57	0.23 × 0.23	0.57	NA	35.19	Yes
[4]	1.57	0.23 × 0.23	1.9	0.38	27.96	Yes
[5]	3.82	0.76 × 0.76	0.62	0.18	1.81	Yes
[6]	2.61	0.21 × 0.19	1.28	0.7	19.45	Yes
[7]	1.49	0.27 × 0.27	0.53	NA	12.51	Yes
Prop.	2.23	0.16 × 0.20	2.60	0.54	56.08	No

parallel combination of capacitor C_F and inductor L_F. The additional capacitor C_C is due to the coupling between ENG-TL radiator and the backside TIF. The complete antenna dimensions are L = 27, $L_f = L_1$ = 7, L_g = 4, L_i = 7, L_2 = 20, $L_3 = L_4 = L_5$ = 4.8, L_6 = 4.5, W = 22, $W_f = W_2$ = 3, W_g = 8, W_1 = 11.4, W_3 = 2, $W_4 = C_R$ = 0.3, L_R = 10, and G_2 = 0.3 (All dimension are in mm). The radiator antenna provides a measured IBW of (2.201–2.259 GHz) 2.60% and simulated IBW of (2.206–2.266 GHz) 2.68% as shown in Figure. 4(a). The proposed antenna provides ARBW ranges from (2.22–2.23 GHz) 0.44%, as shown in Figure. 4(a). The gain plot depicted in Figure. 4(b) shows the highest gain value of 2.54 dBi is obtained at 2.25 GHz. The radiation efficiency is more than 97% for the entire band, as depicted in Figure. 4(b). Figure. 5 shows the antenna can provide right-handed CP (RHCP) radiation in +*Z* direction and left-handed CP radiation in -*Z* direction at 2.23 GHz.

For an electrically small antenna (ESA), Chu proposed the Chu limit, which defines the smaller limit on quality factor (Q_{min}) and maximum attainable bandwidth (FBW_{max}) [2, 13]. After that, Mc Lean provide a revised form for Q_{min} and FBW_{max} explained re-explained in [2], i.e. $Q_{min} = 1/k^3a^3 + 1/ka$ and $FBW_{max} = (S-1)/(Q_{min}\sqrt{S})$, where S is the VSWR. The maximum realizable gain of the ESA is computed using Harrington bound [13] given as $G_{dBi} = 10\log_{10}((ka)^2 + 2ka)$. For the proposed antenna, consider the ENG-TL part excluding the partial ground plane, i.e., 21 mm × 19 mm, a = 14.15 mm and k = 46.07 rad/m at 2.2 GHz. Hence, ka = 0.65. Hence the antenna is electrically small (ka <1). The calculated FBW_{max} = 13.67% and measured bandwidth of 2.68% is obtained. Also, the calculated gain G_{dBi} = 2.36 dBi and simulated gain of 2.54 dBi is obtained which are in acceptable theoretical limits. Table. 1 explain the performance comparison of the intended ENG-TL radiator antenna and existing TL based antennas in *ref.* [3]–[7]. It is observed that the intended radiator antenna provide excellent results.

3 Design of the Intended AMC-MS Reflector

The diagrammatic view of the intended AMC-MS reflector with 4 × 4 unit cell and expanded view of single unit cell is shown in Figure. 6(a). The AMC-MS reflector layer is designed on low-cost FR-4 substrate with thickness H_3 = 3.2 mm, ε_r = 4.4, and tanδ = 0.02. The optimized dimensions are L_a = 2, A_1 = 15.85, A_2 = 4.9, A_3 = 4.19, A_4 = 3.09, A_5 = 1.41, A_6 = 2.82, A_7 = 9.17, A_8 = 4.9, A_9 = 5.77, and g = 0.27 (All dimension in mm). The ±90^0 reflection

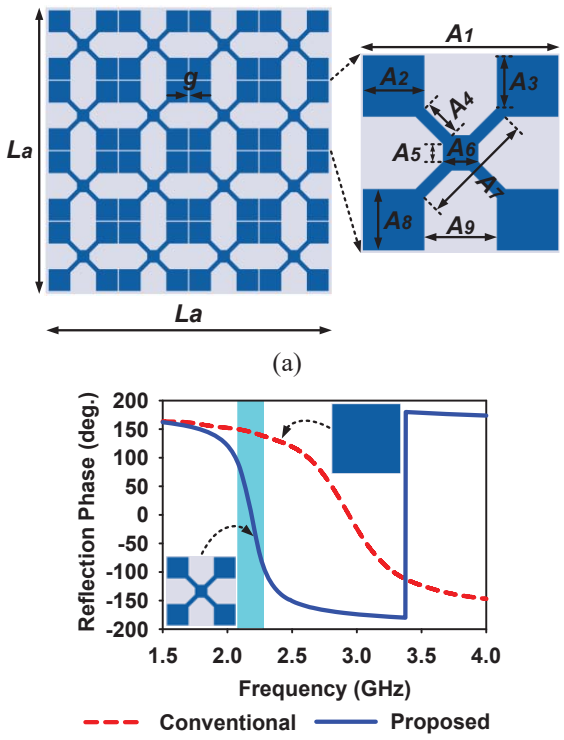

Figure 6. Proposed MS design. (a) Schematic view of the MS reflector, and (b) Reflection phase response

phase of the single MS unit cell with design stages are depicted in Figure. 6(b). The conventional square unit cell provides 0^0 reflection phase at 2.94 GHz, and the proposed MS unit cell provides $\pm 90^0$ reflection phase from 2.07–2.27 GHz with 0^0 reflection phase observed at 2.18 GHz.

4 MS Reflector Loaded Multilayer Antenna

The ENG-TL based CP antenna depicted in Figure. 1 and AMC-MS shown in Figure. 6(a) is combined to form a three-layer structure. The front-view and top-view of the final antenna is depicted in Figure. 7(a) and (b). The upper layer consists of ENG-TL based CP radiator antenna; the middle is the air layer ($\varepsilon_r = 1$); and the lower layer is the MS reflector, which reduces the back lobe and enhances front-to-back ratio of the radiator antenna. The AR and gain response of the MS antenna is plotted with various θ and ϕ values for 2.2 GHz is depicted in Figure. 8(a) and (b). The highlighted portion in the graph shows that the gain values

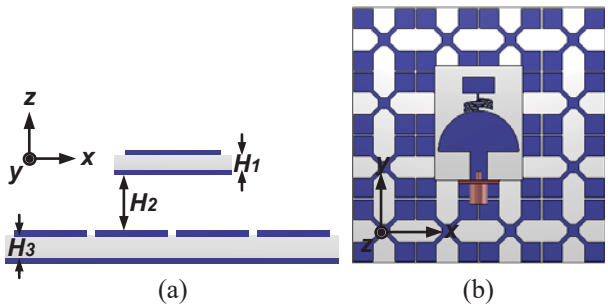

Figure 7. Schematic view of the final multilayer antenna. (a) Side-view and (b) Top-view

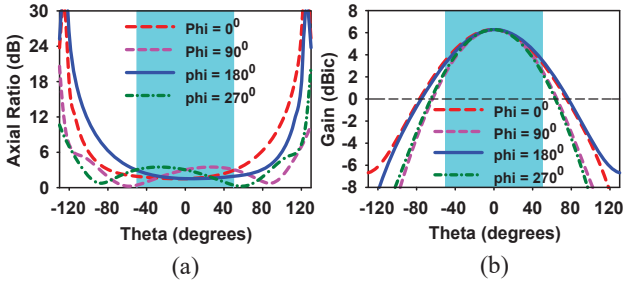

(a) (b)

Figure 8. Proposed MS antenna simulated results at 2.2 GHz. (a) AR performance for $\theta = \pm 50^0$ and $\phi = 0^0$ to 360^0, and (b) Gain performance for $\theta = \pm 50^0$ and $\phi = 0^0$ to 360^0.

are better than 2.04 dBic and approximate AR values less than 3 dB is obtained for $\theta = \pm 50^0$ (AR beamwidth = 100^0) and $\phi = 0^0$ to 360^0 for 2.2 GHz.

5 Results and Discussions of Final Antenna

The $|S_{11}|$ responses with and without MS reflector is shown in Figure. 9(a). The antenna without MS provides an IBW of (2.206–2.266 GHz) 2.68% and with MS (2.16–2.253 GHz) 4.22%. The AR response is also depicted in Figure. 9(a), which ranges from (2.22–2.23 GHz) 0.44% and (2.19–2.22 GHz) 1.36% without and with MS reflector. The simulated gain plot is depicted in Figure. 9(b) provides a gain of 6.33 dBic and 2.18 dBic with and without MS reflector loading at 2.2 GHz. Also, the radiation efficiency is more than 67% and 97% is observed with and without MS shown in Figure. 9(b). Figure. 10(a) and (b) shows the multilayer antenna provides excellent RHCP radiation in both planes for 2.2 GHz in the broadside direction. Table. 2 explains the performance comparison of the intended MS

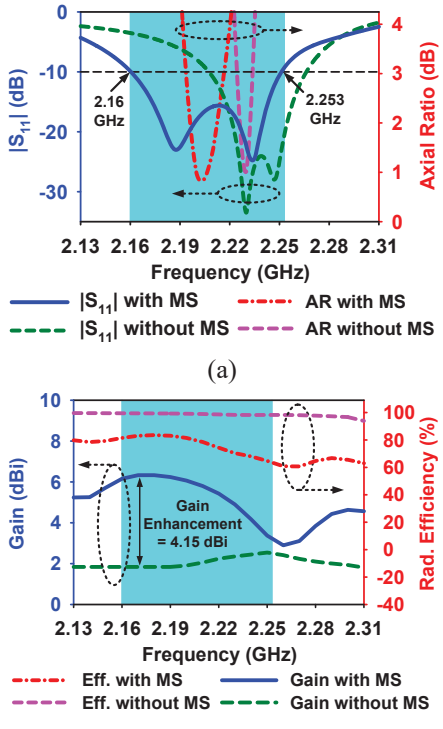

Figure 9. Proposed MS reflector loaded antenna results. (a) $|S_{11}|$ and AR, (b) Gain and efficiency.

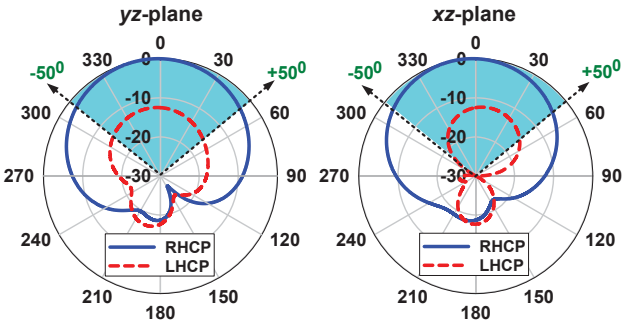

Figure 10. Radiation pattern for *yz* and *xz*-plane at 2.2 GHz

Table 2. Performance comparison of the proposed MS loaded antenna with existing multilayer antenna designs.

Ref. No.	Freq. (GHz)	Overall Antenna Size (mm^3)	Volume (m^3)	Gain (dBi)	G/A Ratio
[8]	2.53	200 × 200 × 8.2	328	3.9	0.86
[9]	1.57	123 × 123 × 9.50	326.7	7	12.1
[10]	1.12	100 × 100 × 21.6	216	2.95	7.49
[11]	1.58	137 × 137 × 82	1539	5.2	6.94
[12]	3.5	100 × 100 × 38	380	3.86	1.80
Prop	2.2	63.4 × 63.4 × 16.2	65.11	6.33	19.9

reflector antenna and existing multilayer antennas in [8]–[12]. The presented AMC-MS antenna provides compact dimensions, lower profile, higher G/A ratio, smaller volume and higher gain than existing designs [8]–[12].

6 Conclusion

A compact ENG-TL CP radiator antenna is combined with MS reflector applicable for airborne application at 2.2 GHz is presented in this work. The antenna compactness and CP radiation are obtained due to the combination of TIF and curved meander lines. The multilayer antenna provides a gain > 2.04 dBic and improved AR beamwidth for AR < 3 dB for $\theta = \pm 50^0$ and $\phi = 0^0$ to 360^0 at 2.2 GHz. The presented antenna results are compared with existing multilayer antennas and observed that the proposed antenna is suitable for providing higher G/A ratio, lower volume, and compact size without any design complexity.

7 Acknowledgements

This research work is supported by Science and Engineering Research Board (SERB), DST, Government of India under grant number EEQ/2016/000023. Also, the authors would like to thank Rogers Corporation for providing Rogers 5880 substrate for fabrication.

8 References

1. M. Ameen and R. K. Chaudhary, "Metamaterial-based circularly polarised antenna employing ENG-TL with enhanced bandwidth for WLAN applications," *Electron. Lett.*, **54**, 20, October 2018, pp. 1152–1154, doi:10.1049/el.2018.5701.

2. M. Ameen and R. K. Chaudhary, "Metamaterial circularly polarized antennas: Integrating an epsilon negative transmission line and single split ring-type resonator," *IEEE Antennas Propag. Mag.*, *early access*, doi: 10.1109/ MAP. 2019.2950920.

3. W. Lin and R. W. Ziolkowski, "Electrically small, low-profile, huygens circularly polarized antenna," *IEEE Trans. Antennas Propag.*, **66**, 2, February 2018, pp. 636–643, doi: 10.1109/TAP.2017.2784432.

4. K. Wei, J. Y. Li, L. Wang, *et. al*, "A new technique to design circularly polarized microstrip antenna by fractal defected ground structure," *IEEE Trans. Antennas Propag.*, **65**, 7, July 2017, pp.3721–3725,doi:10.1109/TAP.2017.2700226.

5. S. Ko, B. Park and J. Lee, "Dual-band circularly polarized patch antenna with first positive and negative modes," *IEEE Antennas Wireless Propag. Lett.*, vol. **12**, 2013, pp. 1165–1168, doi: 10.1109/LAWP.2013.2281320.

6. C. Zhou, G. Wang, *et. al*, "CPW-fed dual-band linearly and circularly polarized antenna employing novel composite right/left-handed transmission-line," *IEEE Antennas Wireless Propag. Lett.*, **12**, 2013, pp. 1073–1076, doi: 10.1109/LAWP.2013.2279689.

7. B. Park and J. Lee, "Omnidirectional circularly polarized antenna utilizing zeroth-order resonance of epsilon negative transmission line," *IEEE Trans. Antennas Propag.*, **59**, 7, July 2011, pp. 2717–2721, doi: 10.1109/TAP.2011.2152337.

8. C. Sim, "Conical beam array antenna with polarization diversity," *IEEE Trans. Antennas Propag.*, **60**, 10, October 2012, pp. 4568–4572, doi: 10.1109/TAP.2012.2207319.

9. J. Lin, *et. al*, "A low-profile dual-band dual-mode and dual-polarized antenna based on AMC," *IEEE Antennas Wireless Propag. Lett.*, **16**, July 2017, pp. 2473–2476, doi: 10.1109/LAWP.2017.2724540.

10. W. Hsieh, *et. al*, "Dual-band circularly polarized cavity-backed annular slot antenna for GPS receiver," *IEEE Trans. Antennas Propag.*, **60**, 4, April 2012, pp. 2076–2080, doi: 10.1109/TAP.2012.2186229

11. L. Wang, H. Yang, and Y. Li, "Design of a new printed dipole antenna using in high latitudes for Inmarsat," *IEEE Antennas Wireless Propag. Lett.*, **10**, April 2011, pp. 358–360, doi: 10.1109/LAWP.2011.2146224.

12. J. Guo, F. Liu, L. Zhao, et. al., "Meta-surface antenna array decoupling designs for two linear polarized antennas coupled in H-plane and E-plane," *IEEE Access*, **7**, July 2019, pp. 100442–100452, doi: 10.1109/ACCESS.2019.2930687.

13. M. Ameen and R. K. Chaudhary, "Electrically small circularly polarized antenna using vialess CRLH-TL and fractals for L-band mobile satellite applications," *Microw. Opt. Technol. Lett.*, **62**, 4, April 2020, pp. 1686–1696, doi: 10.1109/TAP.2011.2152337.